

A nonviral minicircle vector for deriving human iPSC cells

Fangjun Jia¹, Kitchener D Wilson^{1,2}, Ning Sun¹, Deepak M Gupta³, Mei Huang¹, Zongjin Li¹, Nicholas J Panetta³, Zhi Ying Chen⁴, Robert C Robbins⁵, Mark A Kay⁴, Michael T Longaker^{3,6} & Joseph C Wu^{1,6}

Owing to the risk of insertional mutagenesis, viral transduction has been increasingly replaced by nonviral methods to generate induced pluripotent stem cells (iPSCs). We report the use of 'minicircle' DNA, a vector type that is free of bacterial DNA and capable of high expression in cells, for this purpose. Here we use a single minicircle vector to generate transgene-free iPSCs from adult human adipose stem cells.

Nonviral and nonintegrating viral methods for generating induced pluripotent stem cells (iPSCs) using adenovirus¹, plasmids² or excision of reprogramming factors using Cre-*loxP*^{3,4} or piggyBAC transposition⁵ have been reported, but they suffer from low reprogramming efficiencies (<0.003%) and may leave behind residual vector sequences. Recently, human neonatal foreskin fibroblasts have been reprogrammed using episomal vectors derived from the Epstein-Barr virus⁶. However, this technique requires three individual plasmids carrying seven factors, including the oncogene *SV40*, and has not been shown to reprogram cells from adult donors, a more clinically relevant target population. Additionally, expression of the EBNA1 protein, as is required for this technique, may increase immune cell recognition of transfected cells⁷, thus potentially limiting clinical application if the transgene is not completely removed. Protein-based iPSC generation in mouse⁸ and human⁹ fetal and neonatal cells has also been demonstrated but requires either chemical treatment (valproic acid)⁸ or many rounds of treatment⁹. Lastly, protein-based methods necessitate expertise in protein chemistry and handling, which may be unfamiliar to members of some laboratories. Most DNA-based methods require only basic molecular biology background and thus remain a more attractive option for a wider population of researchers interested in cellular reprogramming.

Minicircle vectors are supercoiled DNA molecules that lack a bacterial origin of replication and antibiotic resistance gene; therefore, they are primarily composed of a eukaryotic expression cassette. Compared to plasmids, minicircle vectors benefit from higher transfection efficiencies and longer ectopic expression owing to their lower activation of exogenous silencing mechanisms^{10,11}

and thus may be an ideal strategy for generating iPSCs. We constructed a plasmid (*P2PhiC31-LGNSO*) that contained a single cassette of four reprogramming factors, *POU5F1* (also known as *OCT4*), *SOX2*, *LIN28* and *NANOG*, plus a *gfp* reporter gene, each separated by sequences encoding the self-cleaving peptide 2A (ref. 12) (Supplementary Fig. 1a,b). We next took advantage of the PhiC31-based intramolecular recombination system that allows the plasmid backbone to be excluded and degraded in bacteria and the minicircle to be purified and isolated as described previously^{10,11} (Supplementary Fig. 1c). We validated expression of individual protein factors in 293FT cells (Supplementary Fig. 2). To determine the reprogramming ability of the minicircle vector, we induced pluripotency in human adipose stem cells (hASCs). hASCs have several advantages over other somatic cell types such as fibroblasts as they can be isolated in large quantities (100 ml of human adipose tissue yields about 1×10^6 cells) with minimal morbidity¹³. Furthermore, quantitative PCR (qPCR) analysis of RNA from hASCs revealed three to four times higher relative expression of *KLF4* compared to that in human embryonic stem cells (hESCs) and ~1.3 higher relative expression of *MYC* (also known as *c-MYC*) (Supplementary Fig. 3).

Using hASCs derived from three adults, we introduced the minicircle vector into cells using nucleofection and, as determined by fluorescence-activated cell sorting (FACS), achieved $10.8 \pm 1.7\%$ GFP⁺ cells, compared to only $2.7 \pm 0.8\%$ using a standard plasmid carrying the same expression cassette (Supplementary Fig. 4). We enriched the GFP⁺ cell population 72 h after transfection by flow cytometry and then seeded these cells on inactivated mouse embryonic fibroblast (MEF) feeder layers. Owing to the dilution of the minicircle vector with proliferation, we observed gradual loss of GFP protein and *gfp* mRNA expression in cells that was concurrent with activation of endogenous *OCT4* expression (Fig. 1a). *gfp* expression became essentially undetectable by qPCR analysis by 4 weeks. We performed additional transfections at days 4 and 6 with the minicircle vector to supplement this loss of transgene expression. Compared to standard plasmids that carry a *gfp*-firefly luciferase reporter gene, minicircle DNA with the same reporter gene maintained higher expression for a longer period of time in hASCs, as confirmed by photon counts and qPCR (Supplementary Fig. 5).

On days 14–16, we observed green fluorescent clusters that had morphologic similarities to hESC colonies (Fig. 1b). Many clusters showed no GFP fluorescence at all, suggesting a loss of transgene expression, and we isolated these clusters for subsequent analysis. Similar to hESCs, minicircle-derived iPSC (mc-iPSC) colonies stained positive for embryonic markers (Fig. 1c,d), had reactivated endogenous *OCT4*, *SOX2* and *NANOG*

¹Departments of Medicine and Radiology, ²Department of Bioengineering, ³Department of Surgery, ⁴Departments of Pediatrics and Genetics, ⁵Department of Cardiothoracic Surgery and ⁶Institute for Stem Cell Biology and Regenerative Medicine, Stanford University School of Medicine, Stanford, California, USA. Correspondence should be addressed to J.C.W. (joewu@stanford.edu), M.T.L. (longaker@stanford.edu) or M.A.K. (markay@stanford.edu).

genes (Fig. 1e) and contained increased hypomethylation within the promoters of *OCT4* and *NANOG* compared to that in hASCs (Fig. 1f). Global gene expression profiling of mc-iPSC subclones demonstrated a high degree of similarity to hASCs (Fig. 1g) as well as iPSCs derived using both lentiviral and nonviral vectors (Supplementary Fig. 6). Notably, Southern blot analysis did not detect genomic integration of the minicircle transgene in the subclones (Fig. 1h and Supplementary Fig. 7), and mc-iPSCs had a normal diploid karyotype (Supplementary Fig. 8). We examined the pluripotency of mc-iPSCs both *in vitro* through the formation of embryoid bodies (EBs) and *in vivo* by teratoma formation. EBs expressed genes of all three embryonic germ layers (Fig. 2a) and formed cell types of multiple lineages (Fig. 2b, Supplementary Fig. 9 and Supplementary Video 1). Lastly, subcutaneous injection of each of the three mc-iPSC subclones into immunodeficient mice resulted in a teratoma (Fig. 2c).

In total, we derived 22 mc-iPSC clones from hASCs that had been isolated from three adult donors, yielding an overall

reprogramming efficiency of ~0.005% with minicircle DNA. As with other integration-free iPSC generation approaches, this efficiency is low compared to that of viral methods, which has typically been reported to be ~0.01%^{14,15}. The efficiency we observed with minicircle DNA was still higher than that reported for previous plasmid transfection-based reprogramming methods^{2,6}, though this may be due in part to differences in donor cell types (neonatal fibroblasts versus hASCs¹³) and the number of reprogramming factors used. To address this, we transfected IMR90 neonatal fibroblasts with the minicircle vector and generated iPSCs (as identified by TRA-1-81 immunostaining), though with tenfold lower efficiency (Supplementary Table 1). We could not generate iPSCs using a regular plasmid vector (data not shown); we believe this may be due to the higher transfection efficiency and stronger and more persistent expression of minicircle DNA in cell cultures.

As the reprogramming field moves from basic science toward clinical translation, efficient derivation of iPSCs that are free of

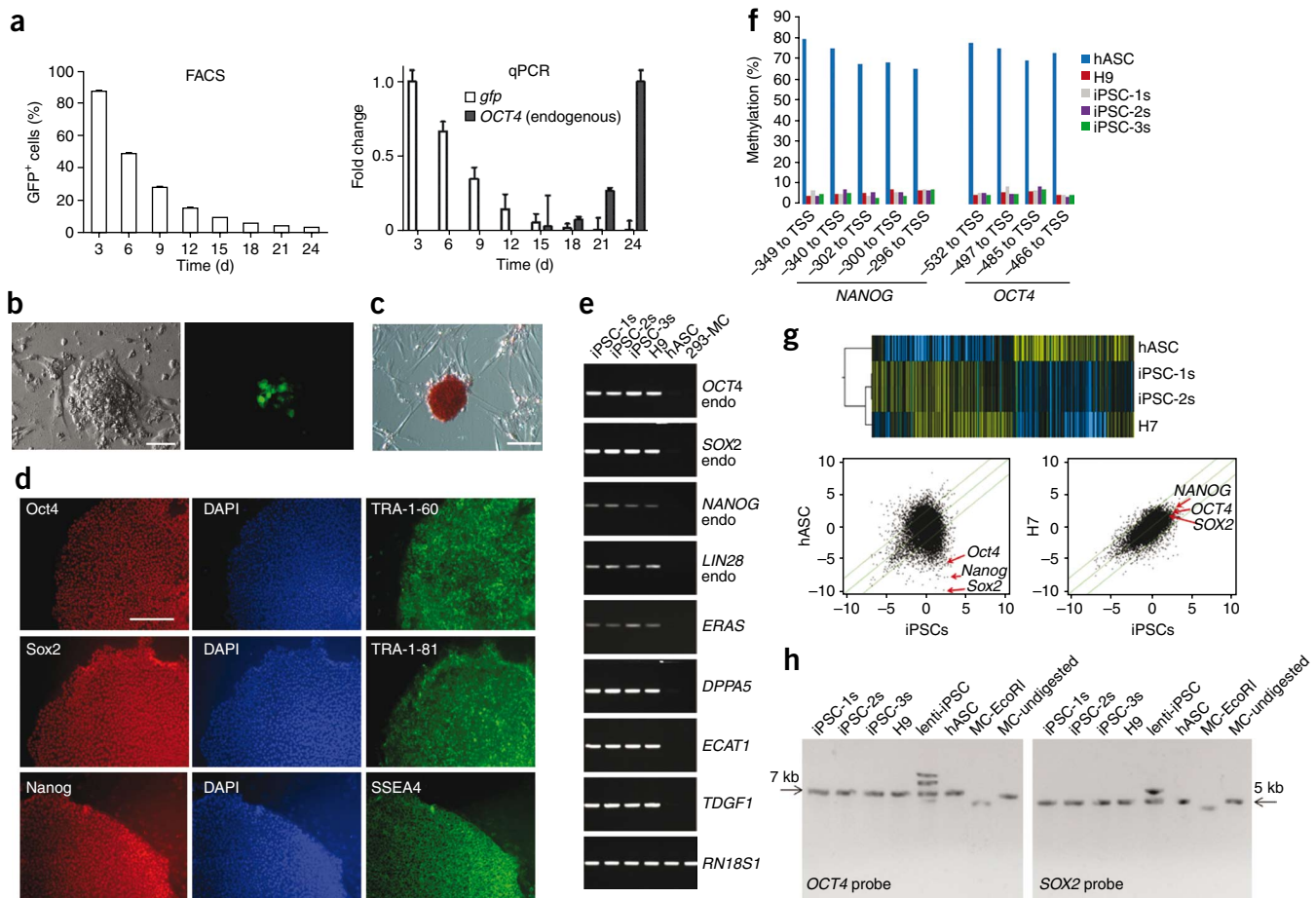
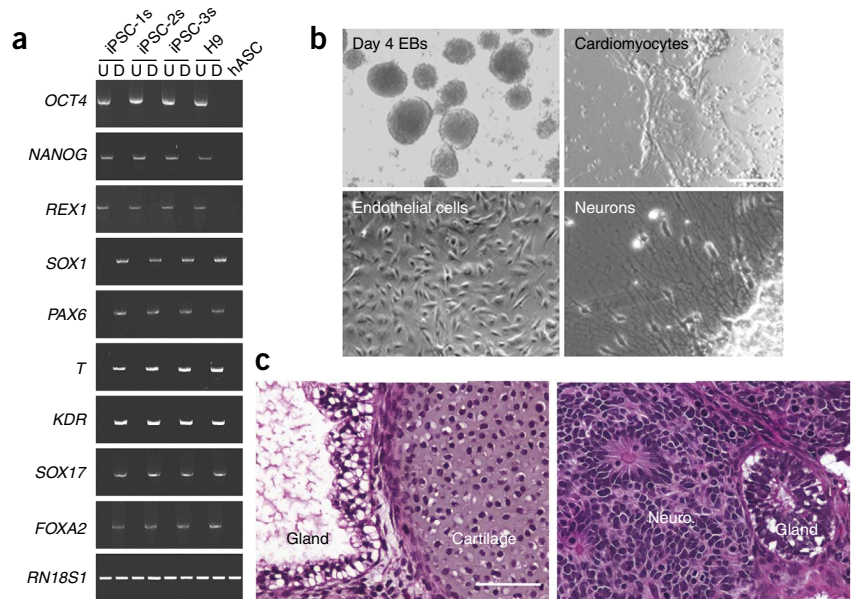


Figure 1 | Generation of iPSCs with minicircle vector. **(a)** FACS and qPCR analysis of hASCs after transfection with the minicircle vector on day 0. Percentage of GFP positive cells (left) and transcript fold change (right) are plotted. Error bars, s.d. ($n = 3$). **(b)** Brightfield (left) and fluorescence (right) images of a day 18 cluster of minicircle-derived iPSCs (mc-iPSCs). **(c, d)** mc-iPSCs stained for alkaline phosphatase **(c)** and immunostained for pluripotency markers **(d)**. Scale bars, 100 μm **(b, d)** and 500 μm **(c)**. **(e)** Reverse transcription-PCR (RT-PCR) analysis of three iPSC subclones (iPSC-1s-3s) derived from three separate donors; H9 hESC line; hASCs; and 293-MC negative control (293FT cells 24 h after transfection with the minicircle vector). Endogenous (endo) *OCT4*, *SOX2*, *NANOG* and *LIN28* were analyzed. *RN18S1* is 18S RNA. **(f)** Bisulfite pyrosequencing measuring methylation in the promoter regions of *OCT4* and *NANOG* in the indicated cells. Distances upstream of transcription start sites (TSS) are indicated in base pairs. **(g)** Heatmap of microarray data (top) and scatter plots depicting gene expression fold changes between paired cell types (bottom; the iPSC data are the average of subclones 1 and 2). Highlighted are *OCT4*, *SOX2* and *NANOG* expression (arrows). Green lines indicate fivefold changes in expression between samples. **(h)** Southern blot analysis of genomic DNA from the indicated cell lines using probes for *OCT4* and *SOX2*. Lenti-iPSC, lentivirally reprogrammed iPSCs as positive control for genomic integration. MC-EcoRI, minicircle vector after digestion with EcoRI; MC-undigested, undigested minicircle vector.

Figure 2 | Pluripotency of mc-iPSCs.

(a) Reverse transcription-PCR (RT-PCR) analysis of undifferentiated (U) and differentiated (D) mc-iPSCs for pluripotency markers (*OCT4*, *NANOG* and *REX1*) and various differentiation markers for the three germ layers (ectoderm, *SOX1* and *PAX6*; mesoderm, *T* and *KDR*; endoderm, *SOX17* and *FOXA2*). (b) Phase-contrast images showing cell types differentiated from mc-iPSCs. (c) Subcutaneous injection of mc-iPSCs caused teratomas in severe combined immunodeficient (SCID) mice. Teratomas consisted of all three embryonic germ layers, including neural tissue (neuro.; ectoderm), cartilage (mesoderm) and glandular structures (endoderm). Representative tissue sections from subclone mc-iPSC-1s are shown. Scale bars, 500 μm (b) and 100 μm (c).



foreign or chemical elements is absolutely critical. Here we describe a nonviral method for generating transgene-free iPSCs from adult donor sources that requires only a single vector without the need for subsequent drug selection or vector excision, or inclusion of oncogenes such as *SV40*. In the future, it will be important to ensure the complete absence of minicircle DNA in therapeutic cells that have been differentiated from mc-iPSCs. Finally, with its basic molecular principles and straightforward protocol, minicircle DNA is ideally suited for facilitating iPSC research.

METHODS

Methods and any associated references are available in the online version of the paper at <http://www.nature.com/naturemethods/>.

Accession codes. Gene Expression Omnibus (GEO): GSE20014 and GSE20033

Note: Supplementary information is available on the Nature Methods website.

ACKNOWLEDGMENTS

We thank A.J. Connolly for assistance with histological analysis, members of the Stanford Functional Genomics Facility and Stanford University PAN Core Facility for assistance with microarrays and A. Cherry for assistance with cytogenetics. We thank funding support from Mallinckrodt Foundation, US National Institutes of Health (NIH) DP2OD004437, HL091453-01A1S109, Burroughs Wellcome Foundation and American Heart Association 0970394N (J.C.W.); NIH R90 DK 07010301, California Institute of Regenerative Medicine T1-00001 and RL1-00662-1, NIH R21 DE018727, RC1HL100490, NIH R21 DE019274, the Oak Foundation and the Hagey Laboratory for Pediatric Regenerative Medicine (M.T.L.); U01HL099776 (R.C.R.).

AUTHOR CONTRIBUTIONS

F.J., K.D.W., N.S., R.C.R., M.A.K., M.T.L. and J.C.W. conceived and designed the experiments. F.J., K.D.W., N.S., D.M.G., M.H., Z.Y.C., Z.L. and N.J.P. performed the experiments. F.J., K.D.W. and J.C.W. wrote the paper.

COMPETING INTERESTS STATEMENT

The authors declare no competing financial interests.

Published online at <http://www.nature.com/naturemethods/>.

Reprints and permissions information is available online at <http://npg.nature.com/reprintsandpermissions/>.

1. Stadtfeld, M., Nagaya, M., Utikal, J., Weir, G. & Hochedlinger, K. *Science* **322**, 945–949 (2008).
2. Okita, K., Nakagawa, M., Hyenjong, H., Ichisaka, T. & Yamanaka, S. *Science* **322**, 949–953 (2008).
3. Kaji, K. *et al. Nature* **458**, 771–775 (2009).
4. Soldner, F. *et al. Cell* **136**, 964–977 (2009).
5. Woltjen, K. *et al. Nature* **458**, 766–770 (2009).
6. Yu, J. *et al. Science* **324**, 797–801 (2009).
7. Munz, C. *et al. J. Exp. Med.* **191**, 1649–1660 (2000).
8. Zhou, H. *et al. Cell Stem Cell* **4**, 381–384 (2009).
9. Kim, D. *et al. Cell Stem Cell* **4**, 472–476 (2009).
10. Chen, Z.-Y., He, C.-Y., Ehrhardt, A. & Kay, M.A. *Mol. Ther.* **8**, 495–500 (2003).
11. Chen, Z.-Y., He, C.-Y. & Kay, M. *Hum. Gene Ther.* **16**, 126–131 (2005).
12. Ryan, M.D. & Drew, J. *EMBO J.* **13**, 928–933 (1994).
13. Sun, N. *et al. Proc. Natl. Acad. Sci. USA* **106**, 15720–15725 (2009).
14. Okita, K., Ichisaka, T. & Yamanaka, S. *Nature* **448**, 313–317 (2007).
15. Wernig, M. *et al. Nature* **448**, 318–324 (2007).

ONLINE METHODS

Minicircle vector. Our minicircle reprogramming vector is available upon request. The sequences of primers used for plasmid construction are listed in **Supplementary Table 2**. The cDNAs for human *OCT4*, *SOX2*, *NANOG* and *LIN28* open reading frames (ORFs) were obtained from human H9 cell line cDNA by PCR. The *gfp* cDNA ORF was cloned from plasmid pmaxGFP (Amaxa). The PCR fragment containing the *NANOG* ORF plus *T2A* sequences was digested with EcoRI and BglII. The PCR fragment containing the *SOX2* ORF plus *T2A* sequence was digested with BamHI and XhoI. The PCR fragment containing the *OCT4* ORF plus *T2A* sequence was digested with SaI and XbaI. These three digested fragments were ligated together and cloned into a modified pUC vector between EcoRI and XbaI sites. The fragment *gfp* ORF plus *T2A*-atgagtgt was digested with EcoRI and NotI and cloned into the vector, as was the PCR fragment containing *LIN28* plus *T2A* sequence that had been digested with SaI and EcoRI. The final vector was designated pUC-LGNSO.

We modified the *P2PhiC31* plasmid by introducing *CMV* promoter and SV40 poly(A) elements as follows. *CMV* promoter was amplified by PCR and a SaI site was added immediately upstream, and XhoI and NotI sites were added downstream, of the promoter. The SV40 poly(A) element was amplified by PCR, and NotI and SpeI sites were added upstream of the element, and XbaI site was added downstream of the element. Both fragments were then ligated together and cloned into *P2PhiC31* between the XhoI and SpeI sites, thus establishing a cloning vector with the required expression elements and XhoI and SpeI cloning sites. Subsequently, the *LGNSO* cassette was retrieved by SaI and XbaI digestion and shuttled into the modified *PsPhiC31* plasmid at the XhoI-SpeI site, creating *P2PhiC31LGNSO* plasmid for minicircle-based reprogramming. The minicircle vector was then purified and isolated as described previously¹¹.

Derivation of human adipose stem cells (hASCs). The phenotype and other characteristics of hASCs have been previously described^{13,16–18}. hASCs were obtained by lipoaspiration after acquiring informed consent from the individuals, in accordance with Stanford University human IRB guidelines. All suction-assisted lipoaspiration procedures were performed using the VASER Lipo System (Sound Surgical Technologies). hASCs were collected from the adipose tissue of male or female individuals between the ages of 40 and 65 undergoing elective lipoaspiration. Participating patients had no prior knowledge or evidence of ongoing systemic disease at the time of operation. All specimens were immediately placed on ice and were washed sequentially in serial dilutions of dilute Betadine, followed by two PBS (pH 7.2) washes of equal volume. Adipose tissues were subsequently digested with an equal volume of 0.075% (wt/vol) type II collagenase in Hank's balanced salt solution (Sigma-Aldrich) at 37 °C in water bath with agitation at 125 r.p.m. for 30 min. After inactivation of collagenase with serum, the stromal vascular fraction was pelleted via centrifugation at 1,200g for 5 min. The cell pellet was resuspended and filtered through a 100 µm cell strainer, and the collected cells were plated on 15-cm dishes for expansion.

Cell culture. hASCs were maintained with Dulbecco's Modified Eagle Medium (DMEM) containing 10% FBS, Glutamax-I, 4.5 g l⁻¹ glucose, 110 mg l⁻¹ sodium pyruvate, 50 units ml⁻¹ penicillin

and 50 µg ml⁻¹ streptomycin at 37 °C, 95% air and 5% CO₂ in a humidified incubator. All cells used for reprogramming were within passage 2. Derived mc-iPSCs were maintained either on MEF feeder layer or on Matrigel-coated tissue culture dishes (ES qualified; BD Biosciences) with mTESR-1 human ES Growth Medium (StemCell Technologies).

Reprogramming hASCs and fibroblasts. Nucleofector Kit R (Amaxa) and program U-023 were used for nucleofection according to the manufacturer's instructions. Transfected cells were plated on 10-cm dishes and cultured in DMEM/F12 medium (Invitrogen) supplemented with 10% FBS. GFP⁺ cells were sorted by flow cytometry 3 d after transfection. The sorted cells were then seeded on gelatin-coated 6-well plates at ~0.5 × 10⁵ cells per well. Cells were switched to hESC culture medium 1 d after seeding, as has been previously suggested¹⁹. Culture medium was refreshed every 2–3 d. On days 4 and 6, we transfected the cells again with minicircle using Lipofectamine 2000 (Invitrogen), which we found to be less toxic than nucleofection. Colonies with morphologies similar to hESC colonies were clearly visible by day 18 after transfection. At day 26–28 after transfection, GFP-negative mc-iPSC colonies were individually picked for further expansion and analysis. For control experiments using a regular plasmid, we used the pUC-LGNSO vector and performed all transfections in parallel with minicircle DNA.

Western blot and immunofluorescence. To examine coexpression of LIN28, NANOG, SOX2 and OCT4, minicircle DNA *LGNSO* was transfected into 293FT cells with Neofectin (Mid-Atlantic Biolabs). Cells were collected for either western blot or immunofluorescence analysis 2 d after transfection. The following primary antibodies were used: rabbit anti-OCT4 (Santa Cruz sc-9081, lot G 0607, 1:500), rabbit anti-SOX2 (Biolegend 630801, lot B115204, 1:500), rabbit anti-NANOG (Cosmo Bio REC-RCAB0004PF, lot T00262-A1, 1:500), rabbit anti-LIN28 (Proteintech 11724-1-AP, lot 2, 1:500) and mouse anti-GAPDH (Millipore MAB374, lot JC1604282, 1:500). Antibodies to hESC surface markers SSEA4 (Millipore MAB4304, lot LV1430331, 1:250), TRA-1-60 (Millipore MAB4360, lot LV1486533, 1:250) and TRA-1-81 (Millipore MAB4381, lot LV1512392, 1:250) were obtained from ES Cell Characterization Kit (Chemicon). Alexa Fluor 488 (Molecular Probes A111029, lot 420004, 1:1,000) and Alexa Fluor 596 (Molecular Probes A11032, lot 419360, 1:1,000) fluorochrome-conjugated secondary antibodies were used for immunofluorescence analysis. Alkaline Phosphatase Detection Kit (Chemicon) was used for alkaline phosphatase staining.

RT-PCR analysis. Total RNA was prepared using RNeasy Mini Kit (Qiagen) and cDNA synthesized with SuperScript II First-Strand Synthesis System for RT-PCR (Invitrogen). PCRs were performed with Taq DNA polymerase (Qiagen). All primer sequences are listed in **Supplementary Table 3**. Note that endogenous genes were measured using 3' untranslated region-specific primers. Quantitative PCR was performed using Taqman Gene Expression Assays (Applied Biosystems) using a StepOnePlus Realtime-PCR System (Applied Biosystems).

Southern blotting. Ten micrograms of genomic DNA was isolated and digested with EcoRI from mc-iPSC subclones derived from each of the three human donors (iPSC-1s, iPSC-2s and

iPSC-3s), H9 hESCs (H9) and hASCs. As positive controls, we included human iPSCs derived from IMR90 fibroblasts using lentiviral transduction methods ('lenti-iPSC'; courtesy J. Thomson, University of Wisconsin), as well as EcoRI-digested and undigested minicircle DNA (8.8 pg starting amounts). After digestion, DNA was separated in 0.8% agarose gel in TAE buffer pH 8.4, then capillary-transferred overnight onto a positively charged BrightStar-Plus nylon membrane (Ambion) in alkaline solution (0.4 N NaOH and 1 M NaCl, pH 12.0). Hybridization was performed using synthesized biotin-labeled probes for either *OCT4* or *SOX2* and detected with the Biostar-BioDetected Kit (Ambion).

Bisulfite pyrosequencing. We used a service provider (EpigenDx). Briefly, 1,000 ng of sample DNA was bisulfite treated using the Zymo DNA Methylation Kit (Zymo Research). The PCR was then performed with one of the PCR primers biotinylated to convert the PCR product to single-stranded DNA templates. The PCR products were sequenced by Pyrosequencing PSQ96 HS System (Biotage) following the manufacturer's instructions. The methylation status of each locus was analyzed individually as a thymine/cytosine single nucleotide polymorphism using QCpG software (Biotage).

Microarrays. Total RNA was prepared from biological duplicate samples of hASCs and H7 hESCs and mc-iPSC subclones from two individuals, for a total of six unique samples. Using Low RNA Input Fluorescent Linear Amplification Kits (Agilent), cDNA was reverse-transcribed from each RNA sample, as well as from a pooled reference control, and cRNA then transcribed and fluorescently labeled with Cy5/Cy3. cRNA was purified using an RNeasy kit (Qiagen). We hybridized 825 ng of Cy3- and Cy5-labeled and amplified cRNA to Agilent 4 × 44K whole human genome microarrays and processed it according to the manufacturer's instructions. The array was scanned using an Agilent G2505B DNA microarray scanner. The image files were extracted using Agilent Feature Extraction software version 9.5.1 applying LOWESS background subtraction and dye normalization. The data were analyzed using GeneSpring GX 10.0 (Agilent Technologies). For heatmap generation, we used ANOVA statistical analysis with multiple testing correction to identify genes that had significant ($P < 0.01$) changed expression between each group; the fold change data for hASC and H7 hESC duplicate samples were averaged for the heatmap. For hierarchical clustering, we used Pearson correlation for similarity measure and average linkage clustering.

Because the majority of microarray data found in the Gene Expression Omnibus (GEO) repository, which is currently the largest fully public gene expression resource, is in the single-color Affymetrix array format, we also performed transcriptional profiling using GeneChip Human Genome U133 Plus 2.0 Arrays (Affymetrix). Total RNA was isolated from three additional mc-iPSC subclones, as described above, and submitted to the Stanford University PAN Core Facility for hybridization and scanning. Using GeneSpring GX 10.0, the resulting data were compared to microarray data published by members of James Thomson's lab for their nonvirally derived human iPSCs⁶ and also to our data for lentivirally derived iPSCs from hASCs¹³ (Supplementary Table 4).

Flow cytometry. FACS analysis and sorting was carried out using a BD LSR analyzer (BD Biosciences) or FACSVantage SEM Flow Cytometry System (BD Biosciences) at the Stanford Shared FACS Facility, and

data were analyzed by FlowJo (Tree Star Inc). Antibodies used in this study were anti-CD31 (BD Pharmingen) for endothelial cell studies; otherwise, cells were sorted by GFP expression. Isotype-matched antibodies were used in flow cytometry for background fluorescence.

Bioluminescence imaging. We constructed a double-fusion reporter gene plasmid (*gfp*-firefly luciferase) driven by a *CMV* promoter and created a minicircle vector from the expression cassette using the techniques already described. *In vitro* imaging of minicircle- or plasmid-transfected hASCs (Supplementary Fig. 5) was performed with the Xenogen *In vivo* Imaging System (Caliper LifeSciences)²⁰. Before imaging, cell medium was removed and D-luciferin (Biosynth AG) and phosphate-buffered saline (PBS) added in a 1:100 ratio. Exposures were taken within 5 min of addition of D-luciferin and then repeated until maximum bioluminescent signal expressed as photons $s^{-1} cm^{-2} sr^{-1}$ was obtained. Three independent experiments were performed.

***In vitro* differentiation.** mc-iPSCs cultured on Matrigel were treated with Collagenase Type IV (Invitrogen) and transferred to ultra-low attachment plates (Corning Life Sciences) in suspension culture for 8 d with DMEM/F12 (1:1) containing 20% knockout serum (Invitrogen), 4.5 g l^{-1} L-glutamine, 1% nonessential amino acids, 0.1 mM 2-mercaptoethanol, 50 units ml^{-1} penicillin and 50 $\mu g ml^{-1}$ streptomycin. EBs were then seeded in 0.25% gelatin-coated tissue culture dish for another 8 d. Spontaneous differentiation of mc-iPSCs into cells of mesoderm, endoderm and ectoderm lineages was then detected by RT-PCR (primers are listed in Supplementary Table 3) and appropriate markers by immunofluorescence. Directed differentiation of mc-iPSCs to cardiomyocytes, neurons and endothelial cells followed previously published protocols^{21–23}.

Teratoma formation. To examine the *in vivo* developmental potential of human iPSCs generated through minicircle DNA-based reprogramming, mc-iPSCs grown on Matrigel-coated dishes were collected by Collagenase IV treatment and injected into the dorsal flank of 6-week-old immunocompromised SCID beige mice (Charles River Laboratories). We injected 0.5×10^6 cells from each of the three donor iPSC lines into individual mice and repeated the experiment a total of three times ($n = 9$ mice total). After 8 weeks, teratomas from all mice were dissected and fixed in 4% paraformaldehyde. Samples were embedded in paraffin and stained with hematoxylin and eosin. All procedures were performed in accordance with protocols approved by the Stanford Animal Research Committee guidelines.

Statistical analysis. Unless otherwise noted, non-microarray data are presented as mean \pm s.d. Data were compared using standard or repeated measures, using ANOVA where appropriate. Pairwise comparisons were performed using a two-tailed Student's *t*-test. For all data, differences were considered significant for $P < 0.05$.

- Bunnell, B.A., Flaat, M., Gagliardi, C., Patel, B. & Ripoll, C. *Methods* **45**, 115–120 (2008).
- Zuk, P.A. *et al. Mol. Biol. Cell* **13**, 4279–4295 (2002).
- Guilak, F. *et al. J. Cell. Physiol.* **206**, 229–237 (2006).
- Huangfu, D. *et al. Nat. Biotechnol.* **26**, 1269–1275 (2008).
- Swijnenburg, R.J. *et al. Proc. Natl. Acad. Sci. USA* **105**, 12991–12996 (2009).
- Osafune, K. *et al. Nat. Biotechnol.* **26**, 313–315 (2008).
- Li, Z. *et al. Stem Cells* **26**, 864–873 (2008).
- Cao, F. *et al. PLoS One* **3**, e3474 (2008).

